Terahertz emission by multiple resonances under external periodic electrostatic field

Divya Singh[1,*] and Hitendra K. Malik[2]
[1]*Department of Physics & Electronics, Rajdhani College, University of Delhi, New Delhi 110015, India*
[2]*PWAPA Laboratory, Department of Physics, Indian Institute of Technology Delhi, New Delhi 110016, India*

(Received 5 June 2019; revised manuscript received 22 January 2020; accepted 4 March 2020; published 17 April 2020)

In the presence of electron neutral collisions of a frequency (ν) of the order of $\nu \geqslant 0.5\omega_p$ (ω_p is the plasma frequency), the collisional effects play an adverse role in the mechanism of terahertz (THz) radiation. The present work describes an approach for the efficient emission of THz radiation with the application of an external periodic electric field in the density rippled collisional plasma wherein an additional transverse component of the current is generated that adds to the THz radiation mechanism. The THz field obtained by coupling of the lasers' field with the external field is termed as an external field induced THz (EFIT). Here, the periodic wave number of the external field enables tuning of the THz radiation and helps achieve multiple resonance conditions for the excitation of large amplitude nonlinear plasma currents.

DOI: 10.1103/PhysRevE.101.043207

I. INTRODUCTION

The present decade is the era of terahertz (THz) technology due to its extensive applications in several realms of life and technologies, viz., imaging, material characterization, topography, tomography, communication, etc. [1,2]. Indeed, there is a basic need to improve upon the efficiency and characteristics of the THz radiation sources and researchers across the globe are consistently working on these issues. In this regard, laser plasma interaction serves as a promising mechanism to generate THz radiation instead of a conventional crystal based mechanism which suffers material breakdown and there is no breakdown limit involved in the plasma. Demir *et al.* [3] have theoretically and experimentally investigated emission of soft x rays from tin plasmas for lithographic application and also calculated the conversion efficiency of the mechanism. Moreover, a large number of studies on various important issues in nonlinear plasma physics including plasma waves, structures, instabilities, and different types of growing waves under the effect of high magnetic field [4–6] have been carried out. Nishida and co-workers [7–9] have demonstrated radiation generation by interaction of a laser pulse with magnetized plasma. We have also investigated THz generation by tunnel ionization of a gas and beating processes [10,11]. Ding and Sheng [12] have obtained few sub-GV/cm THz radiation from relativistic laser-solid interactions via coherent transition radiation, whereas Frolov [13] obtained THz waves by the interaction of a laser pulse with clusters. A cluster has the advantage of having intermediate properties of a solid as well as a gas. Sharma *et al.* [14] have examined the dependence of the shape of nanoparticles on THz emission in the cluster. Miao *et al.* [15] achieved THz radiation generation via resonant transition radiation in inhomogeneous plasmas through laser. On the other hand, González de Alaiza Martínez *et al.* [16] used two color laser pulses at near-relativistic intensities and comparatively studied photoionization and wakefield effects on the generation of THz radiation. A sawtooth wave shaped laser and chirped laser pulses have also been employed for THz emission [17]. Liu *et al.* [18] have obtained enhanced THz wave emission from air plasma by abrupt autofocusing of tailored laser beams. We have also studied THz radiation generation in weakly coupled plasma through wakefield excitation with employment of flat top lasers [19]. Chen [20] has obtained enhanced THz radiation from plasma wakefields via pulse sharpening by a foil shutter. So far, many schemes and approaches have been put forward to enhance THz field amplitude and achieve remarkable efficiency of the order of 6%. It is important to pay attention to the issue of the self-absorption of emitted THz radiation within the medium which is studied by Zhao *et al.* [21] in the preformed plasma. Hence, it becomes imperative to work on these limitations. Sprangle *et al.* [22] formulated a self-consistent model in which a laser pulse partially ionizes the medium, forms a plasma filament, and through the ponderomotive forces associated with the laser pulse, drives plasma currents which are the source of the electromagnetic pulse (EMP), whereas Sun *et al.* [23] have applied an external electric field for obtaining the enhanced THz field amplitude. Wang *et al.* [24] succeded in achieving controllable far-infrared electromagnetic radiation from plasma by applying external dc or ac bias electric fields and Chen *et al.* [25] characterized THz emission from a dc-biased filament in air. On the other hand, Houard *et al.* [26] observed strong enhancement of THz radiation from laser filaments in air by the use of a static electric field. In a different approach based on a dc to ac radiation converter (DARC) frequency upconversion is observed by rapid plasma creation [27] and further frequency is upshifted by dc magnetic field [28], but there is an issue with the conversion of a uniform static electric field interacting with a transversely polarized superluminal ionization front. Our conceptual approach in this article is different from DARC in the context of the tunable

*dsingh@rajdhani.du.ac.in

resonant excitation of nonlinear plasma currents. In addition, Manouchehrizadeh and Dorranian [29] studied the effect of obliqueness of an external magnetic field and investigated relativistic effects [30] in the interaction of a high intensity ultrashort laser pulse with collisional underdense plasma. Singh and Malik [31] have made use of super-Gaussian (sG) lasers for strong THz emissions in collisional plasma. The above works reveal that the laser pulse profile is an important tool for controlling ontrol plasma dynamics and there is a need to devise a technique to harness the energy of plasma waves as a novel radiation source from THz to x-ray range and beyond. In the connection, Kostin and Vvedenskii [32] studied THz emission via self-induced generation of THz emitting plasma currents by laser field and forced generation by a static electric field. Bystrov *et al.* [33] analyzed terahertz radiation of plasma oscillations excited upon the optical (axicon) breakdown of a gas in the presence of external fields and have shown that the spectra and intensity of oscillations and radiation generated by them depend strongly on the character of the spatiotemporal evolution of the formed plasma. Kostin's and Bystrov's approaches are different from the one mentioned in Refs. [22–24,27] in the sense that the THz emission is caused by excitation of the longitudinal current on the superluminous ionization front due to the action of the ponderomotive force of a laser beam. On the contrary, in our approach the plasma is preformed and a highly focused laser incident onto the plasma interacts with the external field via ponderomotive force; henceforth THz emission is caused by the excitation of transverse plasma currents. In the present article, we propose to apply a *spatially* periodic electrostatic field to preformed plasma and use sG lasers for realizing controllable ponderomotive force and, hence, the controlled THz radiation emission. In our approach, the radiating mode of plasma currents is excited at the resonant frequency of the mechanism which can be tuned with the help of period of density ripple (α) and period of electrostatic field (δ). The frequency of a generated radiation spectrum rather depend on the collision frequency and wave number phase matching through resonance. We solve the electromagnetic wave equation under a fast phase variation method to examine the characteristics of emitted electromagnetic radiation which is associated with the excitation of ponderomotive force driven nonlinear plasma currents. In the present paper Sec. II deals with electron oscillatory velocity and ponderomotive force; plasma currents and THz radiation by phase matching are discussed in Secs. III and IV, respectively. Finally, efficiency is described in Sec. V and the Conclusion is presented in Sec. VI.

II. ELECTRON OSCILLATORY VELOCITY AND PONDEROMOTIVE FORCE

We consider two linearly polarized (polarization along the y axis) super-Gaussian (sG) lasers of electric field $\vec{E}_{jL}$, frequency ω_j, and wave number k_j, propagating along the $\vec{z}$ direction in rippled density plasma where weak electron neutral collisions are present. The density ripples of preformed plasma are mathematically expressed as $N' = N_\alpha e^{i\alpha z}$ together with N_α as the amplitude and α the wave number of the density ripples. Presently there are several techniques available for

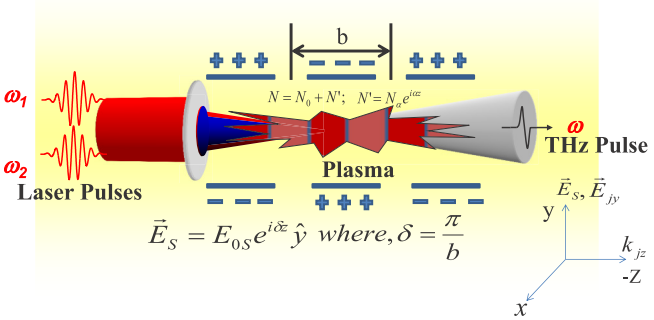

FIG. 1. Schematic of THz radiation generation in the presence of a periodic electric field via laser-plasma interaction.

producing density ripples using a transmissive ring grating and a patterned mask where ripple parameters are controlled for adjusting the period and size of the ripple. A periodic electric field $\vec{E}_s$ (periodicity along the z direction) of wave number δ is applied to the plasma such that its direction is the same as the lasers' polarization (y direction), given as

$$\vec{E}_s = E_{0s} \exp\left[i(\delta_{0s} z - \omega_{0s} t)\right]\hat{y}, \tag{1}$$

where $\omega_{0s} = 0$ and $\delta_{0s} = \delta = 2\pi/2b$ are the angular frequency and wave number of the applied periodic electric field, respectively. We assume that the general exponential form of Eq. (1) is used for mathematical ease from which the real part can be segregated for further analytical calculations such as $E_s = E_{0s}\cos(\delta_{0s} z - \omega_{0s} t) + i\sin(\delta_{0s} z - \omega_{0s} t)$. A similar spatially periodic field with no time dependence is also represented by Higashiguchi *et al.* [28] in their experiment to observe frequency upshift from DARC. This spatially periodic electrostatic field will lie along the direction of polarization of the laser, i.e., the y direction; however, the periodicity lies along the propagation axis, i.e., the z direction. It is interesting to note that there is no comparison between the period of the external electric field (δ) and the rippled density plasma (α) though they are independent but equivalent parameters which may enable tuning of the resonance condition by matching of wave numbers; see Eqs. (16)–(18). It is an essential condition for achieving the maximum transfer of laser energy to terahertz radiation resonantly through the plasma medium to ensure larger amplitudes of emitted terahertz radiation.

The schematic of the mechanism is explained in Fig. 1 and the plasma dynamics is explained with the onset of laser (laser field $\vec{E}_{jL}$) incidence along the z axis onto the preformed rippled plasma as per the equation of motion $m\frac{\partial \vec{v}}{\partial t} = -e\vec{E} - mv\vec{v}$, imparting the oscillatory velocity to the plasma electrons as

$$\vec{v}_j = \frac{e\vec{E}}{m(i\omega_j - \nu)}, \tag{2}$$

where $\vec{E} = \vec{E}_{jL} + \vec{E}_s$ is the sum of the lasers' field and the external periodic field. The field profile of the sG laser is taken as $\vec{E}_{jL} = E_{0L} e^{-(y/b_w)^p} e^{i(k_j z - \omega_j t)}\hat{y}$ where p is the sG index, E_{0L} is the lasers' field amplitude, b_w is the beam width of the laser for full width at half maximum (FWHM), and $j = 1, 2$ corresponds to the sG laser ($p > 2$) and the Gaussian

laser ($p = 2$). Two copropagating lasers are autofocused by an optical lens in the z direction so that these lasers beat in preformed plasma. In view of the high frequency of lasers, only electrons respond to the lasers. Hence, the kind of gas is not so important. In said process, for the resonant excitation of a THz wave, the period of density ripples and the external electric field help out. As such there is no comparison of these periods but they have to satisfy the condition on wave numbers as presented in Eqs. (17)–(18) corresponding to the currents $\vec{J}_2$ and $\vec{J}_3$.

In the presence of an external periodic electric field, a nonlinear ponderomotive force is realized not only at the usual beat frequency $\omega = \omega_1 - \omega_2$ and wave number $k = k_1 - k_2$ but also at modified frequency (ω_1, ω_2) and wave number (k_2', k_3') due to the coupling of the lasers' field with the external electric field, respectively. This ponderomotive force is obtained as

$$\vec{F}_p^{NL} = \frac{e^2}{2m(i\omega_1 - \nu)(i\omega_2 + \nu)} \times \vec{\nabla}[\vec{E}_1 \cdot \vec{E}_2^* + \vec{E}_1 \cdot \vec{E}_s^* + \vec{E}_2^* \cdot \vec{E}_s + \vec{E}_s \cdot \vec{E}_s^*]. \quad (3)$$

Both lasers have different frequency and wave number but the same field amplitudes such that $\omega_1 = 2.4 \times 10^{14}$ rad/s, $\omega = 1.05\,\omega_p$, and $\omega_p = 2.0 \times 10^{13}$ rad/s which yields ω_2 values. With the onset of lasers incidence onto the plasma, the simultaneous mechanism of beat wave enabled THz radiation and external field induced (EFI) THz radiation takes place on the order of few femtoseconds. Therefore, it becomes evident to achieve resonance for which we need resonance controlling parameters and this purpose is served by the period of the external electric field and rippled density plasma. From Eq. (3), mathematically it is clear that the ponderomotive force may have four components, where the first term is due to the beating of lasers in plasma; the second and third terms represent the ponderomotive force caused by the coupling of the first and second lasers' fields with external periodic field, which we may call external field induced (EFI) ponderomotive force. The last term is a nonoscillatory component that does not contribute to the ponderomotive force and hence is superfluous. Therefore, the resultant transverse components of the ponderomotive force, which are responsible for the THz emission are written as

$$F_{py}^{NL} = \left(F_{py}^{NL}\right)_{\text{beating}} + \left(F_{py_1}^{NL}\right)_{\text{EFI}} + \left(F_{py_2}^{NL}\right)_{\text{EFI}}. \quad (4)$$

The magnitudes of both EFI ponderomotive forces are the same but oscillate with different frequencies and wave numbers. The resultant magnitude of these components of ponderomotive force is shown in Fig. 2 with the lines marked as "F_pNL EFI". On the other hand, the line marked as "F_pNL beating" represents the first term of Eq. (4). The magnitude of the beating enabled ponderomotive force is much larger than the EFI ponderomotive force. However, the nature of these forces remains the same; i.e., both components are oscillatory in nature and symmetric about the axis of propagation but the former oscillates with beat wave number and beat frequency, whereas the latter oscillates with modified wave number and laser frequency. Under the effect of these forces, the electron oscillations become nonlinear creating density perturbations due to the redistribution of electrons in the plasma that result in the excitation of nonlinear plasma currents. The EFI ponderomotive force gives rise to EFI THz (EFIT) radiation in addition to the beating enabled THz radiation.

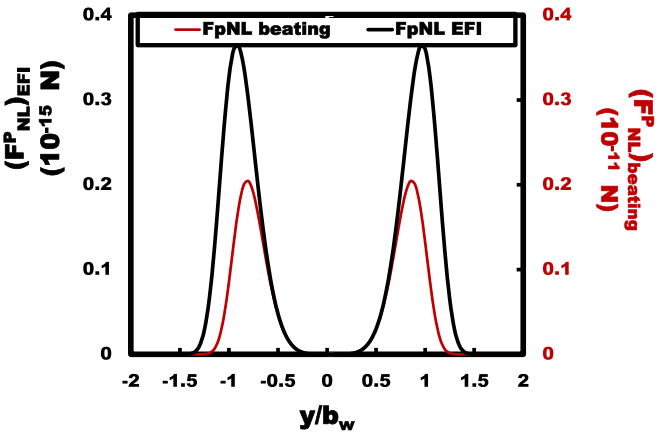

FIG. 2. Transverse components of ponderomotive force with normalized distance from beam axis when $\omega = 1.05\,\omega_p$, $\omega_1 = 2.4 \times 10^{14}$ rad/s, $\omega_p = 2.0 \times 10^{13}$ rad/s, $p = 6$, $\nu = 0.05\,\omega_p$, $E_0 = 5.0 \times 10^8$ V/cm, $E_s = 1.0 \times 10^3$ V/cm, and $b_w = 0.01$ cm; FpNL beating and FpNL EFI represent the first term and resultant of the last two terms of Eq. (4), respectively.

III. STUDY OF DIFFERENT KINDS OF PLASMA CURRENTS

Under the influence of ponderomotive force, the electrons in the collisional plasma acquire the nonlinear velocity $\vec{v}^{NL}$, given by $\vec{v}^{NL} = \frac{\vec{F}_p^{NL}}{m(\nu - i\omega)}$. Corresponding nonlinear and linear density perturbations are obtained as $N^{NL} = \frac{N_0}{m\omega(\omega + i\nu)}\vec{\nabla} \cdot \vec{F}_p^{NL}$ and $N^L = -\frac{\chi_e N_0 e\vec{\nabla}\cdot\vec{\nabla}\phi}{m\omega_p^2}$, respectively, using the continuity equation. It is noteworthy to mention that the linear density perturbations are generated due to the space charge potential (ϕ) which is developed due to linear charge separation and hence linear force is also caused by $\vec{F}_p^{NL}$ which is calculated from the Poisson's equation and expressed as

$$\vec{F}^L = e\vec{\nabla}\phi = \frac{\omega_p^2 \vec{F}_p^{NL}}{i\omega(1 + \chi_e)(\nu - i\omega)}. \quad (5)$$

Finally, the resultant transverse nonlinear electron velocity under the combined action of linear force $\vec{F}^L$ and nonlinear force $\vec{F}_p^{NL}$ is evaluated as $\vec{v}_y' = \frac{i\omega}{m[\omega(\omega + i\nu) - \omega_p^2]}\vec{F}_{py}^{NL}$, which yields the oscillatory nonlinear current density,

$$\vec{J}^{NL} = -\tfrac{1}{2}N' e\vec{v}_y', \quad (6)$$

where $N' = N_\alpha e^{i\alpha z}$ is the ripples in the plasma density. Substituting $Q = \frac{\omega}{[\omega(\omega + i\nu) - \omega_p^2]}$ in the expression of ponderomotive force, we get the following components of the nonlinear plasma current density expressed by Eqs. (7)–(9) which will depend on k_{T1}, k_{T2}, and k_{T3}, [see Eqs. (16)–(18)], respectively, for phase matching that governs which of them will prevail via resonance. Components of the plasma currents

follow:

$$J_{1y}^{NL} = -\frac{1i}{4}\frac{N_\alpha e^3 E_{0L}^2}{m^2(i\omega_1-\nu)(i\omega_2+\nu)}\frac{2p}{b_w}\left(\frac{y}{b_w}\right)^{p-1} \times \exp\left[-2\left(\frac{y}{b_w}\right)^p\right] e^{i\{(k+\alpha)z-\omega t\}}Q, \quad (7)$$

$$J_{2y}^{NL} = -\frac{1i}{4}\frac{N_\alpha e^3 E_{0L}E_{0s}}{m^2(i\omega_1-\nu)(i\omega_2+\nu)}\frac{p}{b_w}\left(\frac{y}{b_w}\right)^{p-1} \times \exp\left[-\left(\frac{y}{b_w}\right)^p\right] e^{i\{(k_1+\alpha-\delta)z-\omega_1 t\}}Q, \quad (8)$$

$$J_{3y}^{NL} = -\frac{1i}{4}\frac{N_\alpha e^3 E_{0L}E_{0s}}{m^2(i\omega_1-\nu)(i\omega_2+\nu)}\frac{p}{b_w}\left(\frac{y}{b_w}\right)^{p-1} \times \exp\left[-\left(\frac{y}{b_w}\right)^p\right] e^{-i\{(k_2-\alpha-\delta)z-\omega_2 t\}}Q. \quad (9)$$

It is obvious that the components J_{1y}^{NL}, J_{2y}^{NL} and J_{3y}^{NL} oscillate at different frequencies and wave numbers. The current density J_{1y}^{NL} is the current generated due to the lasers' beating which is resonantly excited with the help of tuning obtained based on the density ripples in the plasma. On the other hand, the current density J_{2y}^{NL} is excited at frequency ω_1 resonantly by tuning of density ripples and the wave number of the periodic electric field E_s. Similarly the current J_{3y}^{NL} is excited at ω_2. Conclusively, the mechanism of generation of different kinds of plasma currents can be resonantly excited by achieving the phase matching condition based on the tuning of α and δ.

It can be understood in more detail, as both incident lasers are different but have the same amplitude and profile of the field. When lasers are incident on the plasma, they beat together and also produce ponderomotive force to the electrons through their interaction with the static electric field, where they seem to be treated independently. As a result plasma electrons are under the influence of lasers' fields as well as the external electric field. In Eqs. (8) and (9) both wave numbers are different and are nonswitchable. These wave numbers are matched to achieve corresponding resonance with the help of the density ripple parameter and the periodic field wave number, which is the unique aspect of the process that talks about an additional parameter to control and tune resonance.

Figure 3 demonstrates the transverse profile of the external field induced (EFI) plasma currents (combination of J_{2y}^{NL} and J_{3y}^{NL}) and the beat wave induced plasma current J_{1y}^{NL} for sG lasers of index $p = 6$. It is evident that the magnitude of the beating enabled current is much larger than the EFI plasma current, likewise the ponderomotive force. However, the oscillatory nature of both currents remains the same and symmetrical nonlinear currents are generated about the axis of propagation with the employment of sG lasers. The peaks of these currents stay at different positions because these plasma currents oscillate with a different wave number than the ponderomotive force. Hence, tuning of wave numbers must be achieved. The advantage of a periodic electric field is to provide another tunable parameter (δ) besides α, for the purpose of achieving resonance by phase matching that

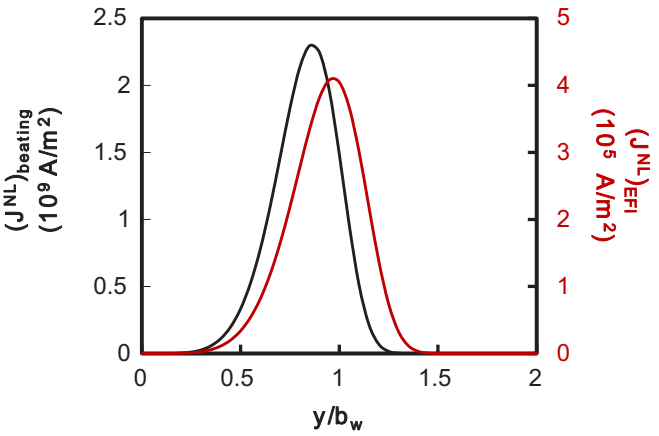

FIG. 3. Transverse profile of plasma currents J_{1y}^{NL} and EFI plasma currents (combination of J_{2y}^{NL} and J_{3y}^{NL}) when $b_w = 0.01$ cm, $\omega = 1.05\,\omega_p$, $\omega_1 = 2.4 \times 10^{14}$ rad/s, $\omega_p = 2.0 \times 10^{13}$ rad/s, $E_0 = 5.0 \times 10^8$ V/cm, $E_s = 1.0 \times 10^3$ V/cm, $p = 6$, and $\nu = 0.05\,\omega_p$.

enables tuning of amplitude and frequency of emitted THz radiation.

In the present case we employed sG lasers which have much less spatial spread, and therefore generate a large amount of ordered nonlinear currents to a good extent responsible for the coherent THz radiation. This observation is consistent with Vvedenskii and Gildenburg [34]. They observed a linear-parametric mechanism of a direct conversion of an ultrashort laser pulse into terahertz radiation due to the ionization induced excitation and the subsequent electromagnetic emission by the axicon focused few-cycle and multicycle laser pulses. For a former pulse with an optimum carrier-envelope phase, the considered mechanism is found much more effective because of ponderomotive-force-induced excitation but for a latter pulse it was ineffective, the reason being a very strong spatiotemporal spread in the initial phase of electron oscillations resulting in a drastic decrease in the ordered electron current for the case of a multicycle laser.

IV. PHASE MATCHING CONDITION AND THz RADIATION FIELD

The nonlinear currents caused by the beating of laser pulses in the plasma are the primary plasma current, and EFI plasma currents are secondary in nature. The former oscillates with frequency $\omega = \omega_1 - \omega_2$ and wave number $k_1' = k_1 - k_2 + \alpha$ whereas the latter oscillates with frequencies and wave numbers ω_1 and $k_2' = k_1 - \delta + \alpha$, and ω_2 and $k_3' = -k_2 - \delta + \alpha$, respectively. The phase matching condition of the beat wave enabled process of THz emission obtained by our group [18,20,31] is reproduced below;

$$\left(\frac{\alpha c}{\omega_p}\right) = \frac{\omega}{\omega_p}\left\{\left[1 - \frac{\omega_p^2}{\omega(\omega+i\nu)}\right]^{\frac{1}{2}} - 1\right\}. \quad (10)$$

However, the phase matching conditions for EFI enabled THz emission process are obtained as

$$\left(\frac{\alpha c}{\omega_p}\right) = \frac{\omega}{\omega_p}\left\{\left[1 - \frac{\omega_p^2}{\omega(\omega + i\nu)}\right]^{\frac{1}{2}} - (k_1 - \delta)\frac{c}{\omega}\right\}, \quad (11)$$

$$\left(\frac{\alpha c}{\omega_p}\right) = \frac{\omega}{\omega_p}\left\{\left[1 - \frac{\omega_p^2}{\omega(\omega + i\nu)}\right]^{\frac{1}{2}} - (-k_2 + \delta)\frac{c}{\omega}\right\}. \quad (12)$$

These electromagnetic fields are excited inside the plasma but may propagate; i.e., the radiation will come out of the plasma. The field of terahertz radiation is calculated using the wave equation of the electromagnetic wave in the plasma, which is obtained with the help of Maxwell's equation under the fast phase variation method where higher order derivatives are neglected. The wave equation is

$$-\nabla^2 \vec{E}_{\mathrm{THz}} + \vec{\nabla}(\vec{\nabla} \cdot \vec{E}_{\mathrm{THz}}) = -\tfrac{4\pi i\omega}{c^2}\vec{J}^{NL} + \tfrac{\omega^2}{c^2}\varepsilon\vec{E}_{\mathrm{THz}}.$$

THz field amplitude in the plasma is in the transverse direction and has y dependence such as $\vec{E}_{\mathrm{THz}} = E_{0y}(y)\exp[i(k_T z - \omega_T t)]\hat{y}$; on satisfying the wave equation we get

$$-\nabla^2 E_{0y} + \frac{\partial}{\partial y}\left(\vec{\nabla} \cdot \vec{E}_{0y}\right) = -\frac{4\pi i\omega}{c^2}J_y + \frac{\omega^2}{c^2}\varepsilon E_{0y}.$$

Assuming the fast phase variation of the THz field in order to neglect higher order derivatives, we get the following component of the THz field (called $E_{0\mathrm{THz}}$):

$$-2ik_T\frac{\partial E_{0\mathrm{THz}y}}{\partial z} + k_T^2 E_{0\mathrm{THz}y} - \frac{\omega^2}{c^2}\varepsilon E_{0\mathrm{THz}y} = -\frac{4\pi i\omega}{c^2}J_{0y}^{NL}.$$

Using the above equations, we get

$$-2ik_T\frac{\partial E_{0\mathrm{THz}y}}{\partial z} + [k_T^2 - \frac{\omega^2}{c^2}\varepsilon]E_{0\mathrm{THz}y} = -\frac{4\pi i\omega}{c^2}J_{0y}^{NL}.$$

Further details can be found in Ref. [31]. We obtain the expression for the amplitude of emitted THz radiation by substituting the expressions of current density $\vec{J}^{NL}$. The amplitude of the beat wave enabled primary THz radiation is obtained as

$$E_{0\mathrm{THz}1} = \frac{2\pi\omega z}{k_{T1}c^2}\frac{1i}{4}\frac{N_\alpha e^3 E_{0L}^2}{m^2(i\omega_1 - \nu)(i\omega_2 + \nu)}\frac{2p}{b_w}\left(\frac{y}{b_w}\right)^{p-1} \times \exp\left[-2\left(\frac{y}{b_w}\right)^p\right]Q. \quad (13)$$

However, the amplitude of EFI enabled secondary THz radiations are given by

$$E_{0\mathrm{THz}2} = \frac{2\pi\omega z}{k_{T2}c^2}\frac{1i}{4}\frac{N_\alpha e^3 E_{0L}E_{0s}}{m^2(i\omega_1 - \nu)(i\omega_2 + \nu)}\frac{p}{b_w}\left(\frac{y}{b_w}\right)^{p-1} \times \exp\left[-\left(\frac{y}{b_w}\right)^p\right]Q, \quad (14)$$

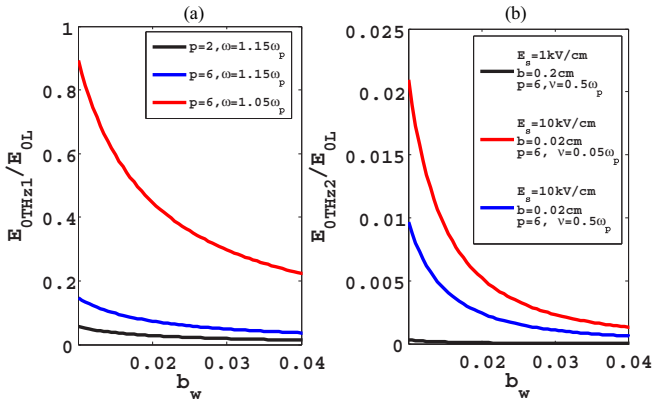

FIG. 4. Variation of normalized amplitude of emitted THz radiation field (a) beat wave enabled THz radiation and (b) EFI THz radiation with beam width for various sG laser profiles and normalized beat wave frequency, when $\omega_1 = 2.4 \times 10^{14}$ rad/s, $\omega_p = 2.0 \times 10^{13}$ rad/s, $E_0 = 5.0 \times 10^8$ V/cm, $y = 0.8\,b_w$, and $\nu = 0.05\,\omega_p$.

$$E_{0\mathrm{THz}3} = \frac{2\pi\omega z}{k_{T3}c^2}\frac{1i}{4}\frac{N_\alpha e^3 E_{0L}E_{0s}}{m^2(i\omega_1 - \nu)(i\omega_2 + \nu)}\frac{p}{b_w}\left(\frac{y}{b_w}\right)^{p-1} \times \exp\left[-\left(\frac{y}{b_w}\right)^p\right]Q. \quad (15)$$

The wave numbers of emitted THz radiations are obtained through phase matching conditions, Eqs. (10)–(12), expressed as k_{T1} for beat wave enabled THz radiation and k_{T2} and k_{T3} are for EFI THz in the following manner:

$$k_{T1} = k_1' = k_1 - k_2 + \alpha, \quad (16)$$

$$k_{T2} = k_2' = k_1 - \delta + \alpha, \quad (17)$$

and

$$k_{T3} = k_3' = -k_2 + \delta + \alpha. \quad (18)$$

A. Comparison of beat wave enabled THz and external field induced THz fields

Figure 4 makes a comparative analysis of normalized amplitudes of beat wave enabled THz radiation and the EFI THz radiations with beam width (b_w) of the lasers. b_w is the beam width of the laser for full width at half maximum (FWHM) which is taken as 0.1 mm (0.01 cm) which is much lower as compared to the other investigators who have taken it in the range of a few centimeters [32–34]. For the smaller beam width a more focused laser gives rise to larger magnitude of ponderomotive force and hence the stronger terahertz radiation. It is seen from Fig. 4(a) that the normalized amplitude of beat wave enabled THz radiation reduces with the increased beam width of the laser. However, this decay can be compensated with the employment of sG lasers of higher index (larger values of p). Moreover, keeping the parameters close to the resonance will give the largest amplitude of emitted

THz radiation. This observation is consistent with what we have obtained in the case of THz generation by laser beating in collisional plasma [18]. González de Alaiza Martínez *et al.* [15] obtained 2% efficiency of the THz mechanism by using multiple-frequency laser pulses to obtain a waveform which optimizes the free electron trajectories in such a way that they acquire the largest drift velocity, whereas in our approach sG lasers are used to generate a large amount of ponderomotive force and nonlinear current densities to ensure 6% efficiency of the THz radiation generation mechanism in magnetized collisional plasma [31].

On the other hand, it is clear from Fig. 4(b) that normalized amplitude of EFI THz radiation also exhibits similar behavior with the beam width, but the magnitude of EFI THz amplitude is significantly lower than that of beat wave induced THz radiation. Further, the EFI THz amplitudes are found to increase with the field strength of an external periodic electric field.

It is to understand that the spectra and intensity of emitted terahertz radiation depends on the spatial evolution of plasma dynamics with laser pulse envelope propagation in the plasma. Precisely, the frequency spectrum of THz radiation is governed by phase matching conditions which brings the frequency range from $\omega - \Delta\omega$ to $\omega + \Delta\omega$, where ω corresponds to the peak frequency of emitted terahertz (primary beat wave enabled resonance) in collisional plasma with bandwidth $2\Delta\omega$. The spectral range $\Delta\omega$ will be decided by the factor of how far we will be able to achieve the secondary (external field induced resonance) resonance condition in the plasma with the tuning of δ and α in conjunction with Eqs. (10)–(12) and (16)–(18). The central frequency and the width of the THz spectrum are determined by the electron collision frequency and can be controlled by changing the spatial period (δ) and ripple period (α). This inference is in agreement with Ref. [32].

B. Role of external periodic electric field

The effect of the strength of an external electric field on the amplitudes of emitted EFI THz radiation is further clarified in Figs. 5 and 6.

Figure 5 shows the impact of separation between electrodes (b) with employment of sG lasers ($p = 6$) and Gaussian lasers ($p = 2$) on the mechanism of EFI THz radiation. When the plate separation is 0.02 cm for the sG laser, a maximum amplitude of EFI THz is obtained that shows linear dependence on the strength of an external periodic electric field whereas larger separation of the order of 0.2 cm does not serve the purpose. Once again it is proven that the sG lasers are far better than the conventional Gaussian lasers for the THz radiation generation. The reason for large amplitude EFI THz radiation for smaller separation between the electrodes (b) may be related to the fact that we are close to the resonance condition and hence, maximum transfer of the momentum takes place between the lasers and the plasma. Moreover, it is obvious that the ponderomotive force carries larger strength in the case of higher periodic field E_s. This leads to the generation of stronger nonlinear current in the plasma (Fig. 6), which causes the emission of stronger THz radiation. If the electrode separation is brought to the nanometer level, it may

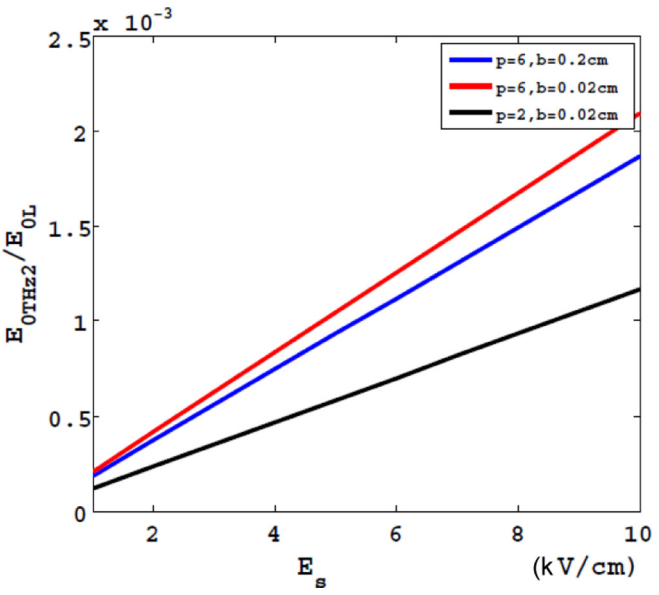

FIG. 5. Variation of normalized magnitude of emitted EFI THz radiation field with external periodic electric field for sG laser when $\omega = 1.05\,\omega_p$, $\omega_1 = 2.4 \times 10^{14}$ rad/s, $\omega_p = 2.0 \times 10^{13}$ rad/s, $E_0 = 5.0 \times 10^8$ V/cm, $y = 0.8\,b_w$, and $\nu = 0.05\,\omega_p$.

do wonders in the field of THz radiation generation via laser plasma interaction.

The increment in the magnitude of ponderomotive force, plasma currents, and EFI THz with an external static electric field follow the same trend as observed by Loffler *et al.* [35], where they reported the generation of THz pulses by photoionization of electrically biased air at 120 kV/cm and the enhancement reported was much less than that reported by our group at 30 kV/cm in the present paper which is more pronounced in the case of sG lasers. Varshney *et al.* [36] also analyzed normalized THz field amplitude with applied external electric field by the beating of two transversely modulated Gaussian laser beams in a plasma at the intensity up to 80 kV/cm, which is a much higher field as compared

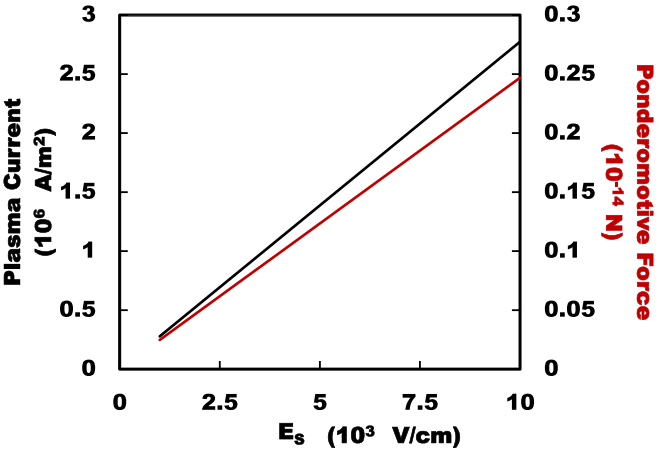

FIG. 6. Variation of EFI plasma currents and ponderomotive force with strength of periodic electric field for sG laser of $p = 6$ when $\omega = 1.05\,\omega_p$, $\omega_1 = 2.4 \times 10^{14}$ rad/s, $\omega_p = 2.0 \times 10^{13}$ rad/s, $E_0 = 5.0 \times 10^8$ V/cm, $y = 0.8\,b_w$, and $\nu = 0.05\,\omega_p$.

to the one used in the present scheme. A similar observation was also made by Sun *et al.* [23] to check the external electric field control of THz pulse generation in ambient air, whereas Chen *et al.* [25] characterized THz emission from a dc-biased filament in air. In all the above mentioned comparative studies, beat wave enabled THz radiation is characterized but in the present approach, with the application of a periodic external static electric field, we obtain a highly specific external field induced (EFI) THz radiation which never had been reported earlier. In fact, we can enhance this field by properly matching the wave numbers k_{T2} and k_{T3} and a broader spectrum of THz radiation may be obtained.

According to Sprangle and co-workers [22] the duration of emitted electromagnetic pulse (EMP) in air, at a fixed point, is a few hundred femtoseconds, i.e., the laser pulse duration plus the electron collision time. The spatial gradients associated with the laser pulse envelope as well as electron collisions lead to ponderomotive forces on the plasma electrons. These forces cause the electrons to oscillate, setting up plasma currents. In our scheme, we employed sG lasers which have large spatial gradients associated with the envelope, finally exciting a large amount of ponderomotive force, hence setting up huge plasma current. The axial and transverse components of plasma currents have oscillatory frequencies close to the beat frequency of the laser pulses. In general the various field components of the plasma oscillations are coupled to induce plasma current which is a source of the THz radiation; however, the plasma currents decay rapidly behind the laser pulse due to the large electron collision frequency. However, the characteristic frequency of the emitted THz is determined by the laser frequencies and the electron collision frequency, and not by the local plasma frequency, fulfilling the phase matching conditions via resonance. It is interesting to note that the entire mechanism takes place transiently.

V. EFFICIENCY OF SCHEME

The efficiency of the EFI THz mechanism (called η_{EFI}) is defined as the ratio of energy of the EFI THz radiation and the energy of the incident lasers, i.e., $\eta_{\mathrm{EFI}} = \frac{\langle W_{\mathrm{THz}E}\rangle}{\langle W_{LE}\rangle}$. The energy density of the lasers is calculated as $\langle W_{LE}\rangle = \frac{1}{8\pi}\frac{b_w E_{0L}^2}{2^{\frac{1}{p}-1}}\frac{\Gamma 1/p}{p}$, where Γ is the gamma function, while that of the THz field is $\langle W_{\mathrm{THz}E}\rangle = \frac{1}{8\pi}\frac{2pE_{0\mathrm{THz}2}^2}{b_w}\frac{\Gamma(2-1/p)}{2^{2-\frac{1}{p}}}$. Based on this, the efficiency η_{EFI} of the mechanism of generation of THz radiation is obtained as

$$\eta_{\mathrm{EFI}} = \left[\frac{2\pi\omega z}{k_T c^2}\frac{1i}{4}\frac{pN_\alpha e^3 E_{0s}}{m^2(i\omega_1-\nu)(i\omega_2+\nu)}Q\right]^2 \times \frac{2^{\frac{2}{p}-2}\Gamma(2-1/p)}{\Gamma 1/p}, \tag{19}$$

where all the symbols have their usual meanings.

A large amplitude of EFI THz radiation is realized when the plasma is confined within closely placed periodic electrodes of alternate polarity. Hence, similar enhancement effect on the efficiency η_{EFI} is also expected for the separation of electrodes. The variation of efficiency of the EFI THz radiation mechanism with the magnitude of the external field is shown in Fig. 7. This figure shows a clear enhancement

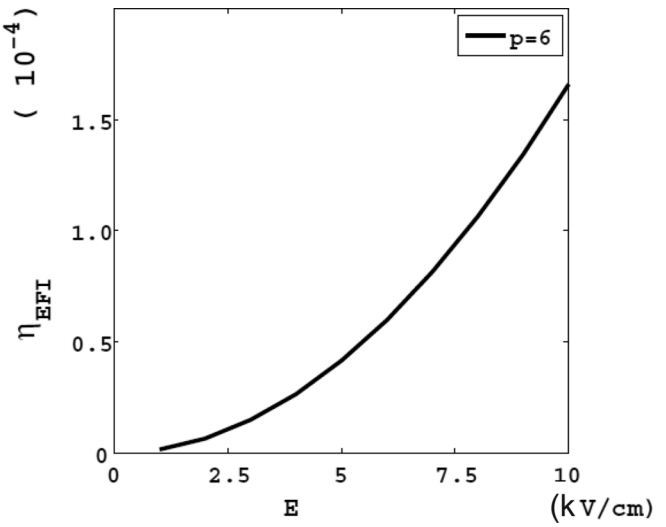

FIG. 7. Variation of efficiency of the mechanism of the generation of EFI THz radiation field with strength of external electric field for sG laser when $\omega = 1.05\,\omega_p$, $\omega_1 = 2.4 \times 10^{14}$ rad/s, $\omega_p = 2.0 \times 10^{13}$ rad/s, $E_0 = 5.0 \times 10^8$ V/cm, $y = 0.8\,b_w$, and $\nu = 0.05\,\omega_p$.

of the efficiency with strength of the external electric field. However, the variation of efficiency η_{EFI} with the field is not linear, unlike the variation of THz amplitude, ponderomotive force, and plasma currents in Fig. 6. The reason is that the efficiency η_{EFI} is directly proportional to the square of the amplitude of the THz radiation.

It is obvious in our case that the plasma is preformed and the laser pulse excites ponderomotive force induced plasma currents in density rippled plasma in the presence of a spatially periodic electric field, whereas in the other approach [33] extraneous static fields serve as a pump to excite natural plasma oscillations and the femtosecond laser pulse served for plasma creation only. Since a considerable fraction of the energy of plasma oscillations is emitted resonantly and their frequencies can be controlled over a wide range by varying the parameters of the rippled density plasma, electric field and laser, our mechanism seems to be promising for generating electromagnetic radiation, certainly in broad terahertz frequency ranges.

VI. CONCLUSIONS

It is concluded that an extra parameter δ is realized besides α to control the tuning of THz radiation in the presence of an external periodic electric field applied to rippled density preformed plasma. In the process, the ponderomotive force is developed due to beating of the lasers as well as by coupling of the lasers' fields with this periodic field. It is important to mention that the efficiency of EFI THz radiation is relatively low as compared to the beat wave excited THz radiation. However, it is a unique approach to excite different amplitudes of THz radiation with matching of the wave numbers.

ACKNOWLEDGMENT

DST and DRDO, Governments of India are gratefully acknowledged for the financial support.

[1] *Opportunities in THz Science*, Report of a DOE-NSF-NIH Workshop held February 12–14, 2004, edited by M. S. Sherwin, C. A. Schmuttenmaer, and P. H. Bucksbaum, https://digital.library.unt.edu/ark:/67531/metadc889765/.

[2] H. T. Chen, W. J. Padilla, J. M. O. Zide, A. C. Gossard, A. J. Taylor, and R. D. Averitt, Nature (London, U. K.) **444**, 597, (2006).

[3] P. Demir, E. Kaçar, E. Akman, S. K. Bilikmen, and A. Demir, Proc. SPIE **6703**, 670301 (2007); P. Demir, E. Kaçar, S. K. Bilikmen, and A. Demir, in *Conversion Efficiency Calculations for Soft X-Rays Emitted from Tin Plasma for Lithography Applications*, edited by C. L. S. Lewis and D. Riley, Springer Proceedings in Physics, Vol. 130 (Springer, Dordrecht, 2009), pp. 281–287.

[4] S. Kawata, Phys. Plasmas **19**, 024503 (2012).

[5] R. Sonobe, S. Kawata, S. Miyazaki, M. Nakamura, and T. Kikuchi, Phys. Plasmas **12**, 073104 (2005).

[6] M. Starodubtsev, Md. K.A. Hassan, H. Ito, N. Yugami, and Y. Nishida, Phys. Plasmas **13**, 012103 (2006).

[7] D. Dorranian, M. Ghoranneviss, M. Starodubtsev, N. Yugami, and Y. Nishida, Phys. Lett. A **331**, 77 (2004).

[8] D. Dorranian, M. Ghoranneviss, M. Starodubtsev, N. Yugami, and Y. Nishida, Laser Part. Beams **23**, 583 (2005).

[9] Y. Nishida and T. Shinozaki, Phys. Rev. Lett. **65**, 2386 (1990).

[10] A. K. Malik, H. K. Malik, and Y. Nishida, Phys. Lett. **375**, 1191 (2011).

[11] R. Gill, D. Singh, and H. K. Malik, J. Theor Appl. Phys. **11**, 103 (2017).

[12] W. J. Ding and Z. M. Sheng, Phys. Rev. E **93**, 063204 (2016).

[13] A. A. Frolov, Plasma Phys. Rep. **42**, 637 (2016).

[14] D. Sharma, D. Singh, and H. K. Malik, Plasmonics **15**, 177 (2019).

[15] C. Miao, J. P. Palastro, and T. M. Antonsen, Phys. Plasmas **23**, 063103 (2016).

[16] P. González de Alaiza Martínez, X. Davoine, A. Debayle, L. Gremillet and L. Bergé, Sci. Rep. **6**, 26743 (2016); P. González de Alaiza Martínez, I. Babushkin, L. Bergé, S. Skupin, E. Cabrera-Granado, C. Köhler, U. Morgner, A. Husakou, and J. Herrmann, Phys. Rev. Lett. **114**, 183901 (2015).

[17] W. M. Wang, Z. M. Sheng, H. C. Wu, M. Chen, C. Li, J. Zhang, and K. Mima, Opt. Express **16**, 16999 (2008).

[18] K. Liu, A. D. Koulouklidis, D. G. Papazoglou, S. Tzortzakis, and X. C. Zhang, Optica **3**, 605 (2016).

[19] D. Singh and H. K. Malik, Nucl. Instrum. Methods Phys. Res., Sect. A **829**, 403 (2016).

[20] Z. Y. Chen, AIP Adv. **6**, 065302 (2016).

[21] J. Zhao, L. L. Zhang, T. Wu, C. Zhang, and Y. J. Zhao, Optics Commun. **380**, 87 (2016).

[22] P. Sprangle, J. R. Peñano, B. Hafizi, and C. A. Kapetanakos, Phys. Rev. E **69**, 066415 (2004).

[23] W. F. Sun, Y. S. Zhou, X. K. Wang, and Y. Zhang, Opt. Express **16**, 16573 (2008).

[24] W. M. Wang, Z. M. Sheng, X. G. Dong, H. W. Du, Y. T. Li, and J. Zhang, J. Appl. Phys. **107**, 023113 (2010).

[25] Y. Chen, T. J. Wang, C. Marceau, F. Theberge, M. Chateauneuf, J. Dubois, O. Kosareva, and S. L. Chin, Appl. Phys. Lett. **95**, 101101 (2009).

[26] A. Houard, Y. Liu, B. Prade, V. T. Tikhonchuk, and A. Mysyrowicz, Phys. Rev. Lett. **100**, 255006 (2008).

[27] N. Yugami, T. Otsuka, Y. Sentoku, A. Nishida, and R. Kodama, in *Proceedings of the 2013 Abstracts IEEE International Conference on Plasma Science (ICOPS), San Francisco, CA* (IEEE, 2013), pp. 1–1.

[28] T. Higashiguchi, N. Yugami, H. Gao, T. Niiyama, S. Sasaki, E. Takahashi, H. Ito, and Y. Nishida, Phys. Rev. Lett. **85**, 4542 (2000).

[29] M. Manouchehrizadeh and D. Dorranian, J. Theor. Appl. Phys. **7**, 43 (2013).

[30] S. Abedi, D. Dorranian, M. E. Abari, and B. Shokri, Phys. Plasmas **18**, 093108 (2011).

[31] D. Singh and H. K. Malik, Plasma Sources Sci. Technol. **24**, 045001 (2015).

[32] V. A. Kostin and N. V. Vvedenskii, New J. Phys. **17**, 033029 (2015); Opt. Lett. **35**, 247 (2010).

[33] A. M. Bystrov, N. V. Vvedenskii, and Gildenburg, JETP Lett. **82**, 753 (2005).

[34] N. V. Vvedenskii and Gildenburg, Phys. Rev. Lett. **98**, 245002 (2007).

[35] T. Loffler, F. Jacob, and H. G. Roskos, Appl. Phys. Lett. **77**, 453 (2000).

[36] P. Varshney, V. Sajal, P. Chauhan, R. Kumar, and N. K. Sharma, Laser and Particle Beams **32**, 375 (2014).